Submitted to Advances in
High Temperature Chemistry

RECEIVED
LAWRENCE
RADIATION LABORATORY

FEB 9 1971

LIBRARY AND
DOCUMENTS SECTION

UCRL-20368
Preprint

c.2

AUGER SPECTROSCOPY ON SURFACES

G. A. Somorjai and F. J. Szalkowski

December 1970

AEC Contract No. W-7405-eng-48

TWO-WEEK LOAN COPY

This is a Library Circulating Copy which may be borrowed for two weeks. For a personal retention copy, call Tech. Info. Division, Ext. 5545

LAWRENCE RADIATION LABORATORY
UNIVERSITY of CALIFORNIA BERKELEY

UCRL-20368 c.2

DISCLAIMER

This document was prepared as an account of work sponsored by the United States Government. While this document is believed to contain correct information, neither the United States Government nor any agency thereof, nor the Regents of the University of California, nor any of their employees, makes any warranty, express or implied, or assumes any legal responsibility for the accuracy, completeness, or usefulness of any information, apparatus, product, or process disclosed, or represents that its use would not infringe privately owned rights. Reference herein to any specific commercial product, process, or service by its trade name, trademark, manufacturer, or otherwise, does not necessarily constitute or imply its endorsement, recommendation, or favoring by the United States Government or any agency thereof, or the Regents of the University of California. The views and opinions of authors expressed herein do not necessarily state or reflect those of the United States Government or any agency thereof or the Regents of the University of California.

AUGER SPECTROSCOPY ON SURFACES

Contents

INTRODUCTION ---------- 1

THE NATURE OF AUGER ELECTRON EMISSION ---------- 3

NOMENCLATURE USED IN AUGER ELECTRON SPECTROSCOPY
AND CALCULATION OF TRANSITION ENERGIES ---------- 7

COMPETING RECOMBINATION MECHANISMS OF VALENCE AND
INNER SHELL ELECTRONS ---------- 10

THE TECHNIQUE OF AUGER ELECTRON SPECTROSCOPY ---------- 13

APPLICATIONS OF AUGER ELECTRON SPECTROSCOPY ---------- 20

ACKNOWLEDGMENTS ---------- 25

REFERENCES ---------- 26

APPENDIX ---------- 28

FIGURE CAPTIONS ---------- 30

FIGURES ---------- 31

AUGER SPECTROSCOPY ON SURFACES

G. A. Somerjai and F. J. Szalkowski

Inorganic Materials Research Division, Lawrence Radiation Laboratory
Department of Chemistry, University of California
Berkeley, California

Introduction

Definitive studies of surface reactions and a variety of other surface properties (vaporization, phase transformation, surface diffusion) require that we obtain detailed information about the atomic surface structure, the chemical composition of the surface, and the concentration of the different surface species at all stages of the experiment. Low-energy electron diffraction studies (the analysis of elastically back-scattered electrons from surfaces) using single crystal surfaces are carried out to determine the atomic surface structure.[1] The analysis of inelastically back-scattered electrons from surfaces that have characteristic energy losses can provide us with qualitative and quantitative analysis of the surface chemical composition. Auger electron spectroscopy (AES), which has recently been developed, analyzes the energy distribution of electrons emitted from a surface following excitation by an incident electron beam of moderate energy (1000-5000 eV). The peaks in the emission spectrum which appear at characteristic energies identify the various surface atoms and from the intensity of the peaks the concentration of a given type of surface atom can be obtained.

Auger electron spectroscopy provides us with a sensitive experimental tool for surface chemical analysis. It is sensitive to the presence of surface atoms in quantities of less than 1% of a monolayer ($\approx 10^{13}$ atoms/cm^2): The analysis is non-destructive; it can be carried out in relatively poor

vacuum ($\leq 10^{-4}$ torr), equally well using crystals, thin polycrystalline foils, powders, or liquids. Qualitative and quantitative surface chemical analysis may be carried out directly on all elements in the periodic table (except hydrogen and helium); the technique is sensitive to atoms of low atomic number, for which X-ray methods can not provide detailed chemical information. One may distinguish between atoms in the surface and bulk atoms using AES. The oxidation states of atoms may be identified by the energy shift of the Auger electron distribuions (chemical shift). In general, AES appears to be sensitive to the chemical environment about surface atoms.

The Nature of Auger Electron Emission

When an energetic beam of electrons or X-rays (1000-5000 eV) strikes the atoms of a material, electrons which have binding energies less than the incident beam energy may be ejected from the inner atomic levels. By this process a singly ionized excited atom is created. The electron vacancy thus formed is filled by de-excitation of electrons from higher electron energy states that fall into the vacancy. The energy released in the resulting electronic transition can, by electrostatic interaction, be transferred to still another electron (in the same atom or in a different atom). If this electron has a binding energy that is less than the de-excitation energy transferred to it, it will then be ejected into vacuum, leaving behind a doubly ionized atom. The electron that is ejected as a result of this de-excitation process is called an Auger electron and its energy is primarily a function of the energy level separations in the atom.[2] In Fig. 1 the Auger mechanism of de-excitation is illustrated in a schematic diagram of the electronic band structure of a typical metallic solid of atomic number Z. The shaded areas represent the filled portions of the bands, three of which have been designated by the generalized notation W_o, X_p, and Y_q with the respective mean energies $-\bar{E}_{W_o}(Z)$, $-\bar{E}_{X_p}(Z)$, and $-\bar{E}_{X_q}(Z)$ relative to the chosen zero of energy, the Fermi energy. ϕ_c is the work function of the crystal. In drawing the schematic diagram it is assumed that an electron vacancy has already been produced in the W_o band. If an electron from the X_p band fills that vacancy, energy of the magnitude $\Delta\bar{E}_{X_p,W_o}(Z) = \{[-\bar{E}_{X_p}(Z)] - [-\bar{E}_{W_o}(Z)]\} = \bar{E}_{W_o}(Z) - \bar{E}_{X_p}(Z)$ is released. If this energy is transmitted to an electron in the Y_q band it must lose $[+\bar{E}_{Y_q}(Z') + \phi_c]$ of energy in order to escape from the crystal; i.e.

the Y_q band electron will be ejected from the atom provided that $[\bar{E}_{W_o}(Z) - \bar{E}_{X_p}(Z)] > [+\bar{E}_{Y_q}(Z') + \phi_c]$. Thus, the binding energy (relative to the vacuum level) of the electron in the Y_q electron band must be smaller than the energy transferred to it in the de-excitation process for Auger electron emission to occur. The emitted electron appears at the collector outside the crystal with the energy

$$\bar{E}_{W_oX_pY_q}(Z) = \bar{E}_{W_o}(Z) - \bar{E}_{X_p}(Z) - \bar{E}_{Y_q}(Z') - \phi_c \qquad (1)$$

relative to the crystal Fermi energy. The term $\bar{E}_{Y_q}(Z')$ has been used instead of $\bar{E}_{Y_q}(Z)$ because the latter refers to the energy level of the singly ionized atom and after the Auger electron is ejected we have essentially a doubly ionized atom.* The Auger electron thus emitted has kinetic energy $\bar{E}_{W_oX_pY_q}(Z)$ that is associated with what is commonly labelled a $W_oX_pY_q$ Auger process.

---

*It has been postulated[2] that $\bar{E}_{Y_q}(Z')$ is the ionization energy of an electron from the Y_q band of the Z^+ ion and so $\bar{E}_{Y_q}(Z') = \bar{E}_{Y_q}(Z+1)$. If we rewrite Eq. (1) as

$$\bar{E}_{W_oX_pY_q}(Z) = \bar{E}_{W_o}(Z) - \bar{E}_{X_p}(Z) - \bar{E}_{Y_q}(Z+\delta) - \phi_c \qquad (1a)$$

where δ is some incremental charge, in most cases the observed Auger energies have been intermediate between those calculated using Eq. (1a) with $\delta = 0$ and $\delta = 1$.

The rate of a particular Auger process is determined by the energy transfer probability between electrons in the various energy levels. It should be emphasized here that the interaction between electrons that participate in the Auger process is essentially electrostatic in nature with theoretical Auger transition probability calculations requiring the evaluation of the transition matrix elements, W_A, of the form[3]

$$W_A = \frac{2\pi}{\hbar} \sum_{i,f} \left| \int\int \psi_f^*(r_1)\, \psi_f^*(r_2)\, \frac{e^2}{|r_1 - r_2|}\, \psi_i(r_1)\psi_i(r_2) dr_1 dr_2 \right|^2 \qquad (2)$$

where $\psi_i(r_1), \psi_f(r_1)$ are the initial and final state wave functions of the first electron, and $\psi_i(r_2), \psi_f(r_2)$ are the initial and final state wave functions of the second electron.

The angular momenta coupling schemes effectively describe the process (even though magnetic interactions do not constitute the driving force for Auger transitions) because the relative electron positions of Eq. (2) which determine the interaction are quantized according to the magnetic fields produced by the electronic spin and orbital angular momenta.

It should be noted that at the present state of development of Auger spectroscopy, the assignment of an $W_o X_p Y_q$ process to an observed transition is tentative since it is based on the agreement obtained when compared with calculated Auger transition energies. The assignment of an experimental peak to an Auger transition can be verified by applying additional experimental tests. These are:[4]

1) Changing the incident electron energy, E_p, across the threshold for ionization of the W_o shell, $\bar{E}_{W_o}(Z)$. The appearance of Auger transitions that appear at $E_p > +E_{W_o}(Z)$ indicate that the W_o shell participates in the Auger process. The experimental Auger electron energy also assists

in determining W_o since $\bar{E}_{W_o X_p Y_q}(Z) < \bar{E}_{W_o}(Z)$.

2) The Auger peak shape and intensity for the same transition can be expected to remain fairly constant for neighboring elements in the periodic table. Therefore, transitions should be assigned to reflect the smooth variation of energy of the core states of neighboring atoms.

3) Peak shape and intensity could be expected to significantly change with changes of chemical state (valency) if one or more valence band electrons are involved in the transition. Such marked changes in the Auger spectrum identify valence electron participation in the transition.

Nomenclature Used in Auger Electron Spectroscopy and Calculation of Transition Energies

An electron orbiting around the nucleus induces a magnetic field, the intensity and direction of which depend on the electron's velocity and orbital radius.[5] There is also an inherent magnetic field associated with an electron, depending on the direction of its spin. The fields produced are commonly referred to as resulting from the orbital angular momentum $\vec{\ell}_i$ and the spin angular momentum, $\vec{s}_i$ of the electron, i. These individual electron spins and angular momenta are vector quantities and their sum gives the total electronic angular momentum, $\vec{j}_i = \vec{\ell}_i + \vec{s}_i$, for an isolated electron. For high atomic number elements, it has been found that the electronic interactions are well described by the sum over the individual $\vec{j}_i$'s to obtain the total atomic angular momentum $\vec{J}_{j-j} = \sum_i \vec{j}_i$. In this case, it is said that the electron-electron interaction obeys j-j coupling and the individual electrons are labelled according to the traditional X-ray spectroscopic notation as follows:

X-ray symbol	Electron energy state	Electron $\vec{j}$
K	1s	1/2
L_1	2s	1/2
L_2	2p	1/2
L_3	2p	3/2
M_1	3s	1/2
M_2	3p	1/2
M_3	3p	3/2
M_4	3d	3/2
M_5	3d	5/2
N_1	4s	1/2
.	.	.
.	.	.
.	.	.

Often, when the binding energies of two electron states are indistinguishable, the X-ray symbols are combined for brevity; e.g., M_4 and M_5 will become $M_{4,5}$. For low atomic number elements, however, the atom is better described if the individual orbital angular momenta are considered to interact together to produce a total orbital angular momentum, $\vec{L} = \sum_i \vec{\ell}_i$. In a like manner for the spin component, we obtain the total spin angular momentum, $\vec{S} = \sum_i \vec{s}_i$. These quantities may then couple together to form the total atomic angular momentum, $\vec{J}_{LS} = \vec{L} + \vec{S}$, in what is known as either the L-S or Russell-Saunders coupling scheme,[6] where a given electron distribution is denoted by a term symbol of the form $^{(2\vec{S}+1)}L_{\vec{J}_{LS}}$. In the atomic number range of approximately 25 to 75,[7] neither scheme adequately describes the atom and it is necessary to combine them into an intermediate coupling description. Due to the availability of the atomic energy levels, from atomic spectroscopy studies the observed Auger transitions are commonly associated with a $W_oX_pY_q$ transition regardless of the atomic number of the element involved. Although this notation is beneficial in that the Auger ejection process can be visualized in terms of the atomic X-ray levels, viewed in the light of the preceding discussion it is misleading for the intermediate and low atomic number elements. An unambiguous treatment would require difficult quantum mechanical calculations of the energy differences between the possible doubly-ionized and singly-ionized states and comparison of these values with the experimental energy. The corresponding notation would designate both the j-j and L-S coupling limits to which the particular Auger process would tend[8]: e.g. $KL_1L_2(^1P_1)$ and $KL_1L_2(^3P_0)$ refer to two different final states of the excited atom which are indistinguishable using the X-ray notation alone.

The following calculation is to show how the $L_2M_{2,3}M_{4,5}$ assignment was made for the experimentally determined 474 eV Auger peak of vanadium. The published X-ray levels in electron volts for vanadium (Z=23) and chromium (Z=24) are[7]

	K	L_1	L_2	L_3	M_1	$M_{2,3}$	$M_{4,5}$
V	5465	628	520	513	66	38	2
Cr	5989	692	584	575	74	43	2

Since the incident beam energy, E_p, was 2500 eV, the initial ionization could not have occurred in the K level. Also, since the ejected Auger electron energy was 474 eV, the ionization could not have occurred in any of the M levels. Calculations using Eq. (6), which is an experimentally modified form of Eq. (1a), were carried out and the results are presented below in the columns labelled Z and Z+1 respectively with those $W_oX_pY_q$ transitions most closely approximating the experimental energy. The analyzer work function, ϕ_A, is approximately 5 eV.

	(Z)	(Z+1)
$L_1M_1M_1$	491	483
$L_2M_1M_{4,5}$	447	447
$L_2M_{2,3}M_{4,5}$	475	475
$L_3M_{2,3}M_{4,5}$	468	468

On the basis of these calculations alone, the $L_2M_{2,3}M_{4,5}$ assignment can be justified. However, if the energy separation between the calculated transitions is not so large as to allow easy distinguishability, similar calculations could be made for Ti (Z=22) and Cr (Z=24) and the transition that exhibits a monotonic energy level variation is singled out.

Competing Recombination Mechanisms of Valence and Inner Shell Electrons

When an electron beam in the range of hundreds to five thousand electron volts impinges on the single crystal surface, more than ninety-five percent of the scattered electrons undergo energy exchange of some type due to interaction with the crystal and its electrons. The 1-5% elastically scattered fraction is that which is used for diffraction studies. The efficiency of the Auger electron emission process depends on the probabilities of other competing inelastic energy transfer processes, between the incident electron beam and the surface atoms. The inelastic scattering mechanisms can be subdivided into two groups. Some of the peaks in the inelastic electron spectra A) shift in energy loss with varying excitation energy, E_p. Most of the peaks however, B) appear at well defined energies that remain unchanged while changing the incident beam energy. These peaks are due to true secondary electrons and solely reflect the energy level structure of the scattering atom.

A) The incident electron beam can undergo energy losses through direct coupling into the lattice vibrations of the solid(phonon excitations).[9] Energy exchange between the electrons and phonons lead to thermal diffuse scattering, and to the Debye-Waller factor in electron diffraction (exponential attenuation of the diffraction beam intensities with increasing temperature.) Heating of the crystal by the electron beam can also take place through phonon excitations although the incident beam intensities which are used in most Auger spectroscopy studies are sufficiently low ($\mu amps/mm^2$) so that there is no appreciable heating effect at surface temperatures above 100°K.

The electrons incident on the surface can also interact with valence electrons and excite them out of the crystal. "Secondary" electron emission due to electron impact is one of the most important primary processes that can take place in the crystal. The ratio of emitted secondary electron current to incident electron current could be quite high for a number of metals (2-3) but very high for several large band gap insulators (20-25) such as aluminum oxide and MgO.[9] The incident electron beam can also cause the buildup of a space charge at the surface of solids with low free carrier concentration which then changes the energy distribution of the incident electron beam. For most insulators, due to the large secondary emission, the surface is positively charged and the electron beam incident on the crystal is further accelerated in the crystal lattice.[10]

B) The incident electron beam could cause direct excitation of plasma oscillation of the free electrons in the crystal. The energy of the surface plasma is on the order of 10 eV and excitation of such correlated oscillation of conduction electrons has been used to study several different electrical properties of surface atoms.[11] The incident electrons, if they are energetic enough to excite the bound electrons in the core states, will excite them with high efficiency. If the electron energy is high enough to observe Auger transitions, several different excitation processes in addition to Auger excitation can take place.[7] The primary excitation processes of inner shell electrons which take place upon electron (or X-ray) beam incidence are the emission of a "photoelectron" from a core state into vacuum or the absorption of the excited shell electron in the conduction band. These are shown in Fig. 2.

The dominant de-excitation process in addition to the Auger electron emission is X-ray fluorescence, i.e. the de-excitation of the atom by emission of electromagnetic radiation. The Auger electron emission involving the K-shell appears to be much more probable for light elements (with atomic number less than 32) than X-ray fluorescence while X-ray emission is the more likely de-excitation process for heavier elements.

Finally, the incident electron beams may also cause chemical reactions at the surface that involve the surface atoms or the absorbed molecules.[1] Such chemical reactions may result in the production of new surface species or desorption and fragmentation of the adsorbed molecules. The chemical interaction of the surface atoms with the incident electron beam may take place since the incident electron beam energies are orders of magnitude greater than the chemical binding energies of the surface atoms. For example, alkali halides (sodium fluoride, lithium fluoride, etc.) were found to decompose in the electron beam.[12] There is halogen evolution under electron impact and the alkali metal may precipitate at the surface. Carbon monoxide chemisorbed on metal surfaces was found to undergo partial decomposition in the electron beam to give a carbon deposit at the surface[13] and to undergo partial desorption as neutral molecules and ions.

Fortunately, the cross sections for electron beam induced surface chemical reactions appear to be quite low for most solids and chemisorbed gases when compared to other excitation processes that may take place. However, all of these energy loss processes between the incident electron and the surface atoms compete with the Auger process. These different mechanisms of energy transfer have to be considered in studying the composition and the chemical nature of the materials using the Auger spectroscopy.

The Technique of Auger Electron Spectroscopy

The Auger electron emission is essentially an atomic property. Although the transition probabilities of the different Auger processes may be modified due to the atomic environment about the emitting atoms (packing, order, etc.). Auger Electron Spectroscopy (AES) for surface chemical analysis can be carried out using crystals, polycrystalline foils, powders, and liquids equally well. Metals, ionic solids, semiconductiors, or insulators may all be used as target materials. Any process that will produce an initial inner shell vacancy will provide the conditions necessary for the ejection of Auger electrons. The poorest vacuum that can possibly be tolerated in Auger studies is the one that will allow sufficient mean free path for electron travel between the incident electron source and the target, and the target and the detector. This is on the order of 10^{-4} torr. More stringent conditions are usually imposed by the requirements of the particular experiment.

The scheme of the apparatus that is used most frequently in Auger spectroscopy studies at present is shown in Fig. 3. The electron beam from a gun that is similar to that used in an oscilloscope is incident on the target surface at approximately 15° incidence with respect to the surface plane.

Accurate quantum mechanical calculation of the ionization cross-section of an atom by an electron is difficult to carry out. However, an estimate using a form of the Born approximation and scaled values of the back-scattering factor have shown that the probability for ionization of an electron in a particular shell should reach a maximum at a primary electron energy of about 3 to 3.5 times the binding energy of the electron

in that shell (i.e. $E_p/E_{shell} \approx 3 \rightarrow 3.5$).[14] This probability is not expected to vary greatly in the range $E_p/E_{shell} = 2.5 \rightarrow 6$. The amount of ionization produced within the escape depth of the Auger electrons can be expected to increase approximately as $\sin^{-1}\theta$ (θ being the angle of incidence with respect to the surface plane) so that a beam incident at a grazing angle should give a larger signal than one at normal incidence. This has been verified[15] by experiments and an optimum angle of incidence of about 15° was established. It should be noted that the incident electron beam does not have to be monoenergetic since its energy does not enter into either calculations of the Auger energy or Auger peak widths. The incident beam merely serves to create the initial electron vacancy through the process of ionization. Calculations predict a total Auger current from the K-shell ionization of oxygen on the order of magnitude of 10^{-11} amps per monolayer for a normal incident primary beam of 1 μA[14] that is spread over an area of 2-3 mm^2. This corresponds to an electron flux on the order of 10^{10} electrons/cm^2 sec which coincides with the magnitude of the current detected by experiments. The emitted electrons are energy analyzed by an assembly of four grids and a collector plate in the retarding field energy analyzer (RFEA) (see Fig. 3). The first and fourth grids are grounded for shielding, and a negative d.c. ramp voltage, upon which a small sinusoidal a.c. modulation ($k \sin\omega t$, k being the amplitude of the modulation and ω its angular frequency) is impressed, is applied to the coupled second and third grids. The electrons that pass through the analyzer are thus modulated at the frequency ω and are collected. This modulated current is then converted to voltage using a sensing resistor and fed into the signal channel of the lock-in amplifier, which is tuned to detect the second harmonic frequency, 2ω. This is done because

the Auger peak is usually located on a steeply sloping background due to other secondary electrons which one finds desirable to cancel out in order to better detect the Auger peak. If a Taylor series expansion of current vs voltage is performed [see the Appendix] we see that the current amplitude at the second harmonic frequency, A_2, is

$$A_2 = \frac{k^2}{4} \frac{d^2I}{dV^2} + \frac{k^4}{48} \frac{d^4I}{dV^4} + \frac{k^6}{1536} \frac{d^6I}{dV^6} + \cdots \qquad (3)$$

and that this amplitude is proportional to the second derivative of the current to the collector (i.e., $A_2 \propto d^2I/dV^2$) provided that the modulation voltage is small enough such that the higher order derivative terms in Eq. (3) are negligible when compared to the second derivative contribution. The current, I, and its derivatives, dI/dV and d^2I/dV^2 are plotted as a function of the voltage schematically in Fig. 4. It can be seen that the derivative signals define well the peak positions.

Assuming that the peak has a normal Gaussian distribution, Taylor[16] has shown that for a peak to peak modulation that is equal to the half width (at half height) of the peak, the maximum error introduced by the higher order derivative contributions to the approximation

$$A_2 \approx k^2/4 \; (d^2I/dV^2) = i \; 0.06 \; (k^2/\sigma^2) \qquad (4)$$

where

σ = standard deviation of Gaussian curve = 0.8475 of the half width at half height

i = total peak current

is less than 6%. The maximum error due to the higher order terms in the first harmonic amplitude, A_1,

$$A_1 \approx k \frac{dI}{dV} = 0.4\ (k/\sigma)\ i \qquad (5)$$

is less than 5% for the same experimental conditions. Although A_1 is larger than A_2 under typical experimental conditions the second harmonic is more easily detected since the rapidly varying background is virtually eliminated and the gain of the detector can be increased. Also, energy losses often cause tailing out of the low energy side of the peak leaving only a high energy edge and therefore making it difficult to establish the position of the peak using the first derivative method. Since the second derivative technique transforms this inflection into a peak, it provides a sharp point at which to measure the transition energy.

Auger electron spectroscopy by the retarding field energy analysis technique is well suited for surface chemical analysis in combination with other techniques of surface studies. In particular it can be carried out in combination with low-energy electron diffraction studies, using the same vacuum chamber, electron optics and collector. The grid system in the LEED "mode" is adjusted to retard the inelastically scattered electrons and allow the penetration of only the elastic component. THe fluorescent screen is used to display the diffraction beams. The same grid system in the Auger "mode" can monitor the energy distribution of inelastic back-scattered electrons and the fluorescent screen is used as a collector to detect the modulated signal. The cylindrical electrostatic analyzers that are also available for AES measurements[17] provide rapid scanning rates that are especially useful in reaction kinetics studies along with several other desirable design features. These advantages however, are traded for lower sensitivity and/or energy resolution. It is of

advantage, nevertheless, to use a separate electron gun at a grazing angle to the surface as a source of incident electrons instead of the LEED gun (which is fixed for normal incidence) in order to obtain maximum ionization in the surface layers of the crystal. In addition, AES can be carried out in combination with ellipsometry, mass spectrometry, work function measurements, diffusion studies, flash desorption analysis, and many other experimental techniques.

We have discussed the method of assignment of experimental Auger peaks by comparing them to calculated Auger transitions. The experimentally determined peak energies must be corrected, however, to account for a slight acceleration or deceleration of the Auger electron on the way to the analyzer due to the contact potential (difference in work functions) between the crystal and the analyzer. As a result, the energy is measured with respect to the analyzer ground and Eq. (1a)[7] becomes

$$\bar{E}_{W_o X_p Y_q}(Z) = \bar{E}_{W_o}(Z) - \bar{E}_{X_p}(Z) - \bar{E}Y_q(Z+\delta) - \phi_A \qquad (6)$$

where ϕ_A is the analyzer work function. That is, the energy will be independent of the work function of the target sample. Depending on the composition of the crystal, however, a space charge may develop at the surface and this will shift the energy of the peak and should be taken into account. Also, there may be broadening and extra peaks appearing on the low energy side of the Auger peak which are due to the characteristic loss mechanisms an electron may undergo in moving through the crystal, i.e., excitation of interband transitions and of plasmons.

The width of the peak will depend on a number of different parameters. I) If Δ_{W_o}, Δ_{X_p}, and Δ_{Y_q} are defined as the widths of the W_o, X_p, and Y_q bands respectively, by insertion into Eq. (6), we obtain the relation for the range of electron energies contained in the Auger peak:

$$E_{W_o X_p Y_q}(Z) = \bar{E}_{W_o X_p Y_q}(Z) \pm \frac{1}{2}(\Delta_{W_o} + \Delta_{X_p} + \Delta_{Y_q}) \qquad (7)$$

Consequently, the maximum width of the Auger peak due to the bandwidths is $(\Delta_{W_o} + \Delta_{X_p} + \Delta_{Y_q})$, which is what one would expect if the variation in the density of states in the bands were ignored. Usually $\Delta_{W_o} << \Delta_{X_p}, \Delta_{Y_q}$ especially if X_p and/or Y_q refer to the valence bands and thus Δ_{W_o} can be neglected. If X_p and Y_q are the same band, then it is possible to calculate the variation of electron density within the band since the observed Auger peak is a weighted function of the density of electronic states.

II) The peaks will also be broadened due to the electron lifetimes in the bands during the transition in accordance with the Uncertainty Principle. Since the electron transition times are on the order of 10^{-16} sec. the Auger peak width is on the order of a few electron volts. [$\Delta E \approx \hbar/\Delta t = (6.6 \times 10^{-16}$ eV-sec$)/10^{-16}$ sec $= 6.6$ eV].

III) The main instrumental effects that contribute to the peak width are[16]:

a) The a.c. modulation. This widens the energy base width of any monoenergetic signal current to the magnitude of the peak-to-peak modulation.

b) The potential variation between the retarding grid wire and the center of the mesh. Experimental values for a single grid are $\Delta V/V \approx 2.5\%$ and for a coupled double grid $\Delta V/V \approx 0.5\%$; that is, the width a monoenergetic signal at 100 eV appears to be 0.5 volts.

c) Work function variations at the retarding grid contribute to ΔE. These have been found to be less than 0.2 eV.

Using Eq. (3), it is possible to obtain an indication of the peak current or intensity since, upon rearranging, we have

$$i = \frac{A_2}{0.06} \frac{\sigma^2}{k^2} = \frac{hd^2}{0.48\ k^2}$$

where h = peak maxima-minima height (in units of current and corrected for amplification)

d = maxima-minima energy separation

That is, the peak intensity is proportional to the peak height times the square of the distance separating the second derivative peaks. For the vanadium 474 eV peak, using a 50 μamp, 2500 eV incident electron beam and a 5 volt peak to peak modulation, typical values of h and d are 2 volts (after amplification) and 8 volts respectively. Since the Auger signal is amplified by approximately 2×10^4 after being converted into a voltage across a 10^6 ohm resistor, $h \approx \frac{(2\ \text{volts})}{(2\times10^4)(10^6\ \text{ohms})} = 10^{-10}$ amp

Therefore, for the 474 eV peak,

$$i \approx \frac{(10^{-10}\ \text{amp})(8\ \text{volts})^2}{(0.48)(2.5\ \text{volts})^2} = 2 \times 10^{-9}\ \text{amps}$$

Harris,[18] using a 127° sector analyzer in measuring the angular distribution of the emitted Auger electrons, showed that the intensities of the substrate peaks approach a cosine distribution but that in some cases the impurity peaks are strongly angle dependent. This raises the possibility of distinguishing atoms which lie mainly on the surface from those which are distributed in the bulk of the substrate. However, the problem of determining the distribution normal to the surface is not easily solved.

Applications of Auger Electron Spectroscopy

Most of the Auger spectroscopy studies of surfaces were carried out for purposes of surface chemical analysis. Figure 5 shows the Auger spectra from the (100) and (110) crystal faces of vanadium and from a polycrystalline vanadium foil. The most distinct feature of the vanadium Auger spectra is the group of peaks in the energy range 375-525 eV. By comparing the peak positions with those calculated from atomic tables and comparing them to Auger transitions of neighboring elements, most of the peaks could be assigned. In addition, carbon and sulfur can easily be detected on the vanadium surface by their Auger transitions at 277 eV, and 150 eV, respectively. Comparison of the Auger spectra from vanadium single-crystal and polycrystalline foil surfaces (Figs. 5a,b,c) indicate that electron spectroscopic data can be obtained from both types of surfaces with approximately equal sensitivity. In Figs. 6a and 6b the Auger spectra from a vanadium surface that is free from adsorbed gases and from the same surface covered with a monolayer of oxygen is compared. Although the intensities of the vanadium Auger peaks are reduced by about 20%, all of the Auger transitions that are due to vanadium atoms are discernible. There is a marked reduction of the intensities of the carbon and sulfur Auger peaks upon gas adsorption; nevertheless, these peaks, which are due to the presence of small concentrations of surface impurities, are still detectable under a monolayer of gas. Thus, Auger surface analysis may be carried out in poor vacuum, if necessary.

Figure 7a and 7b shows the Auger spectra of the V(100) surface before and after heat treatment in vacuum at 1100°C. The sulfur peak increases upon heating, indicating marked surface segregation during

annealing. The carbon peak, on the other hand, appears to diminish, indicating the disappearance of carbon from the surface. Since at the heating temperatures the carbon cannot vaporize from the surface, it is likely to have diffused into the bulk of the vanadium crystal. One can then investigate the thermal history of solids that is so important in determining many of their physical-chemical and mechanical properties. One such study has been reported by Harris.[19] He has analyzed a stainless steel specimen containing 1.6% chromium, 3.5% nickel, 0.39% carbon, and trace amounts of manganese, antimony, tin and phosphorous. The steel was austenitized at 1000 to 1100°C, which dissolved the carbon and enlarged the grain size of the polycrystalline material. The stainless steel was quenched to martensite and then tempered at 650°C after which it was quenched in water. Embrittlement of the ingot occurred when it was heated to 593°C and cooled very slowly during the period of one week. Auger spectroscopy studies indicated that embrittlement to a large extent was due to the diffusion of chromium from the bulk to the surface during the slow cooling period. The increase in the chromium Auger signal could be followed directly as a function of annealing and as a function of embrittlement.

It has been found that, in addition to carbon, sulfur is probably the most tenacious impurity one encounters on metal surfaces. Sulfur can change the properties of several materials, and its removal may be more difficult than that of carbon since its reaction kinetics with oxygen is not as favorable.

Although many different surfaces have been used for Auger spectroscopic analysis, here we mention only a few selected application of Auger spectroscopy to surface analysis. In a series of experiments silicon

surfaces were steam oxidized and the Auger spectra of the silicon peaks were monitored as a function of the oxidation treatment.[20] Upon steam oxidation the peak at 92 V (due to Si atoms) has completely disappeared, indicating that no elemental silicon is present at the steam oxidized surface. Electron bombardment of the oxide surface, however, at 900 V for only 10 minutes caused sufficient decomposition to produce enough elemental silicon that was easily discernible by Auger spectroscopy. Thus, the surface passivation of semiconductors could be directly followed by Auger spectroscopy and its effectiveness could be monitored.

The surface compositions of moon dust brought back by the Apollo flights have been analyzed using Auger spectroscopy.[21] The surface composition underwent marked changes as a function of temperature. Due to ambient contamination of the dust the surface composition below 300°C was similar to that of any other contaminated sample on the earth's surface. Above this temperature, however, the partial decomposition of potassium compounds could be monitored. Such an analysis allows one to correlate the surface composition with mass spectrometry studies of the thermal decomposition products. Several minerals of interesting chemical composition which do not exist on the earth's surface were discovered this way.

Auger spectroscopy, in addition to providing qualitative surface chemical analysis, may also be easily used to provide quantitative chemical analysis. Figure 8a shows Auger spectrum of potassium atoms that are adsorbed on the germanium (111) surface in a fractional monolayer coverage.[22] Figure 8b shows the magnitude of the peak-to-peak intensity of the potassium Auger peak plotted as a function of potassium coverage on the surface.

There is a good linear relationship indicating that the observed intensity could be directly correlated with the amount of impurity adsorbed on the surface if suitable calibration is employed. Gallium arsenide photocathodes have also been subjected to quantitative Auger spectroscopic analysis and it was found that the photoemission from the surface could be correlated with the amount of carbon on the surface which poisons the photo response.[23] The photoemission yield decreased in proportion to the increasing carbon concentration. In fact, upon the deposition of a monolayer of carbon at the surface photoemission ceased completely.

One of the most promising applications of Auger spectroscopy is in the detection of the oxidation state of surface atoms using the "chemical shift" of Auger peaks. Figure 9 shows the Auger peak obtained from sodium thiosulfate[24] which contains two different sulfur atoms in different chemical states with oxidation numbers 6^+ and 2^-. There are two distinct Auger peaks, one shifted with respect to the other, which could be identified as due to the two sulfur atoms of different valency. The observed chemical shift when calibrated to a known reference oxidation state, allows one to identify the oxidation state of the surface atoms that participate in chemical surface reactions or chemisorption.

It has been reported recently that elemental carbon and carbon monoxide can be distinguished on metal surfaces by the variation of the Auger spectra.[25]

It appears that the Auger transition probabilities are very sensitive to the chemical environment about surface atoms. It is hoped that this technique may also be applied to monitor changes in the core electron binding energies as a function of changes of the atomic environment

of surface atoms, i.e., changes of anion or cation in a polyatomic solid, the appearance of impurities on the surface or changes in the defect structure at the surface.

Another use of Auger spectroscopy is the comparison of the surface composition with that of the bulk composition near the surface. As the electron beam penetrates deeper into the material below the first monolayer, it samples several atomic layers below the surface and provides us with bulk chemical information. The signal is limited by the depth from which the Auger electrons can escape without loss of energy. The Auger signal due to bulk atoms could be maximized under conditions of normal incidence. The penetration depth of the incident beam can be changed by changing the angle of incidence from normal to grazing angle of incidence thereby the surface Auger signal could be amplified at the expense of the bulk Auger signal. This way not only the surface composition but its time-dependent changes, that is, in-diffusion or out-diffusion of impurity atoms from the bulk to the surface could also be monitored.

It should be noted that Auger spectroscopy should be eminently useful in studying the surface composition of alloys or solid solutions. Due to the differences in surface free energies of the elements participating in the binary or multi-component systems, it is likely that the surface compositions are different from that of the compositions in the bulk. Accumulation or depletion of one-component at the surface is expected for a number of different alloy systems. This way, surface thermodynamics of multi-component systems could be studied. So far, no attempt has been made to use Auger spectroscopy in studies of surface thermodynamics.

Auger spectroscopy could also be carried out on various catalyst surfaces such as those containing small metal particles dispersed on high surface area carriers (for example alumina), or on zeolites. These studies could be carried out using liquid surfaces. Since Auger electron spectroscopy is a non-destructive, sensitive experimental tool for quantitative and qualitative surface chemical analysis, applicable to materials of various surface morphology, and the measurement can be carried out in relatively poor vacuum, if necessary, it is expected to occupy a role of major importance in various chemical studies in the near future.

ACKNOWLEDGMENT

This work was supported by the U. S. Atomic Energy Commission.

REFERENCES

1. G. A. Somorjai and H. H. Farrell, "Low Energy Electron Diffraction," Adv. Chem. Phys. (to be published).

2. E. H. Burhop, The Auger Effect and Other Radiationless Transitions, The University Press, Cambridge, England (1952).

3. M. A. Listengarten, Bull. Acad. Sci. USSR. Phys. Ser. U.S.A. 26, 182 (1962).

4. T. W. Haas, J. T. Grant, and G. J. Dooley, Phys. Rev. B 1, 1449 (1970).

5. J. L. Eisberg, Fundamentals of Modern Physics, John Wiley & Sons, Inc., New York (1961).

6. G. Herzberg, Atomic Spectra and Atomic Structure, Dover Publications, New York (1944).

7. K. Siegbahn, C. Nordling, A. Fahlman, et al., ESCA: Atomic, Molecular and Solid State Structure Studied by Means of Electron Spectroscopy, Almquist and Wiksalls Boktryckeri AB, Uppsala, Sweden (1967).

8. I. Bergström, C. Nordling, et al., Alpha, Beta, and Gamma Ray Spectroscopy, North-Holland Publishing Co., Vol. II (1965).

0. A. J. Dekker, "Secondary Electron Emission," Solid State Physics, Academic Press, Vol. 6, New York (1958).

10. T. M. French and G. A. Somorjai, J. Phys. Chem. 74, 2489 (1970).

11. H. Reather, J. de Physique 31, C1-59 (1970).

12. H. Tokutaka, M. Prutton, et al., Surface Sci. 21, 233 (1970).

13. A. E. Morgan and G. A. Somorjai, J. Chem. Phys. 51, 3309 (1969).

14. H. E. Bishop and J. C. Rivière, J. Appl. Phys. 40, 1740 (1969).

15. P. W. Palmberg, Appl. Phys. Letters 13, 183 (1968).

16. N. J. Taylor, Rev. Sci. Instr. 40, 792 (1969).

17. Varian Associates; Physical Electronics Industries, Inc.; Vacuum Generators Ltd.

18. L. A. Harris, Surface Sci. 15, 77 (1969).

19. L. A. Harris, J. Appl. Phys. 39, 1428 (1968).

20. C. C. Chang, Surface Sci. (to be published).

21. F. J. Szalkowski and G. A. Somorjai, Science (to be published).

22. R. E. Weber and A. L. Johnson, J. Appl. Phys. 40, 314 (1969).

23. J. J. Uebbing, J. Appl. Phys. 41, 802 (1970).

24. A. Fahlman, K. Hamrin, et al., Physics Letters 20, 159 (1966).

25. T. W. Haas and J. T. Grant, Appl. Phys. Letters 16, 172 (1970).

Appendix

The generalized Taylor series formula is

$$f(x+h) = f(x) + h\frac{df}{dx} + \frac{h^2}{2!}\frac{d^2f}{dx^2} + \frac{h^3}{3!}\frac{d^3f}{dx^3} + \cdots$$

where h is the perturbation on x of which f is some function.

The situation where the current, I, is expanded as a function of a d.c. voltage (V_o) with a.c. modulation $(k \sin \omega t)$ superimposed upon it follows:

$$I(V_o = k \sin \omega t) = I(V_o) + k \sin \omega t \frac{dI}{dV_0} + \frac{k^2 \sin^2 \omega t}{2!}\frac{d^2I}{dV_0^2}$$

$$+ \frac{k^3 \sin^3 \omega t}{3!}\frac{d^3I}{dV_0^3} + \frac{k^4 \sin^4 \omega t}{4!}\frac{d^4I}{dV_0^4}$$

$$+ \frac{k^5 \sin^5 \omega t}{5!}\frac{d^5I}{dV_0^5} + \frac{k^6 \sin^6 \omega t}{6!}\frac{d^6I}{dV_0^6} + \cdots$$

$$= I(V_o) + k \sin \omega t \frac{dI}{dV_0} + \frac{k^2}{2!} + \left(\frac{1-\cos 2\omega t}{2}\right)\frac{d^2I}{dV_o^2}$$

$$+ \frac{k^3}{3!}\left(\frac{3 \sin\omega t + \sin 3\omega t}{4}\right)\frac{d^3I}{dV_0^3}$$

$$+ \frac{k^4}{4!}\left(\frac{3/2 - 2\cos 2\omega t + 1/2\cos 4\omega t}{4}\right)\frac{d^4I}{dV_0^4}$$

$$+ \frac{k^5}{5!}\left(\frac{10\sin\omega t - 5\sin 3\omega t + \sin 5\omega t}{16}\right)\frac{d^5I}{dV_0^5}$$

$$+ \frac{k^6}{6!}\left(\frac{5/2 - 15/4\cos 2\omega t + 3/2\cos 4\omega t - 1/4\cos 6\omega t}{8}\right)\frac{d^6I}{dV_0^6}$$

$$+ \cdots$$

$$= I(V_0) + \left[\frac{k^2}{4}\frac{d^2I}{dV_0^2} + \frac{k^4}{64}\frac{d^4I}{dV_0^4} + \frac{k^6}{2304}\frac{d^6I}{dV_0^6} + \cdots\right]$$

$$+ \left[k\frac{dI}{dV_0} + \frac{k^3}{8}\frac{d^3I}{dV_0^3} + \frac{k^5}{192}\frac{d^5I}{dV_0^5} + \cdots\right]\sin\omega t$$

$$- \left[\frac{k^2}{4}\frac{d^2I}{dV_0^2} + \frac{k^4}{48}\frac{d^4I}{dV_0^4} + \frac{k^6}{1536}\frac{d^6I}{dV_0^6} + \cdots\right]\cos 2\omega t$$

$$- \left[\frac{k^3}{24}\frac{d^3I}{dV_0^3} + \frac{k^5}{384}\frac{d^5I}{DV_0^5} + \cdots\right]\sin 3\omega t$$

$$= I(V_o) + A_0 + A_1\sin\omega t - A_2\cos 2\omega t - A_3\sin 3\omega t + \cdots$$

The following trigonometric relations have been used above:

$$\sin^2\omega t = \frac{1}{2}(1-\cos 2\omega t)$$

$$\sin^3\omega t = \frac{1}{4}(3\sin\omega t - \sin 3\omega t)$$

$$\sin^4\omega t = (\sin^2\omega t)^2 = \frac{1}{4}(\frac{3}{2} - 2\cos 2\omega t + \frac{1}{2}\cos 4\omega t)$$

$$\sin^5\omega t = \frac{1}{16}(19\sin\omega t - 5\sin 3\omega t + \sin 5\omega t)$$

$$\sin^6\omega t = (\sin^2\omega t)^3 = \frac{1}{8}(\frac{5}{2} - \frac{15}{4}\cos 2\omega t + \frac{3}{2}\cos 4\omega t - \frac{1}{4}\cos 6\omega t)$$

Figure Captions

Fig. 1. Schematic representation of the Auger electron emission from a metallic solid containing an electron vacancy in the W_o energy band.

Fig. 2. Schemes of the photoelectron emission and X-ray absorption processes.

Fig. 3. Scheme of the retarding field apparatus used for Auger Emission Spectroscopy.

Fig. 4. Plots of the collected current, I, and its derivatives, dI/dV and d^2I/dV^2, as a function of the retarding voltage, V.

Figs. 5a,b,c. Auger emission spectra from a) the (100), b) the (110) crystal faces of vanadium, and from c) a polycrystalline foil using E_p = 2500 eV.

Figs. 6a,b. Auger emission spectra from a) the gas free, and b) the oxygen covered (100) crystal face of vanadium using E_p = 2500 eV.

Figs. 7a,b. Auger emission spectra from the (100) crystal face of vanadium a) after ion bombardment, and b) after heat treatment at 1100°C in ultrahigh vacuum.

Figs. 8a,b. a) Characteristic Auger emission spectrum of potassium on the germanium surface.

b) The variation of the peak-to-peak intensity of the potassium Auger peak as a function of potassium coverage of the surface.

Fig. 9. Sulfur Auger emission peaks characteristic of the +6 and -2 oxidation states of the sulfur atoms in sodium thiosulfate.

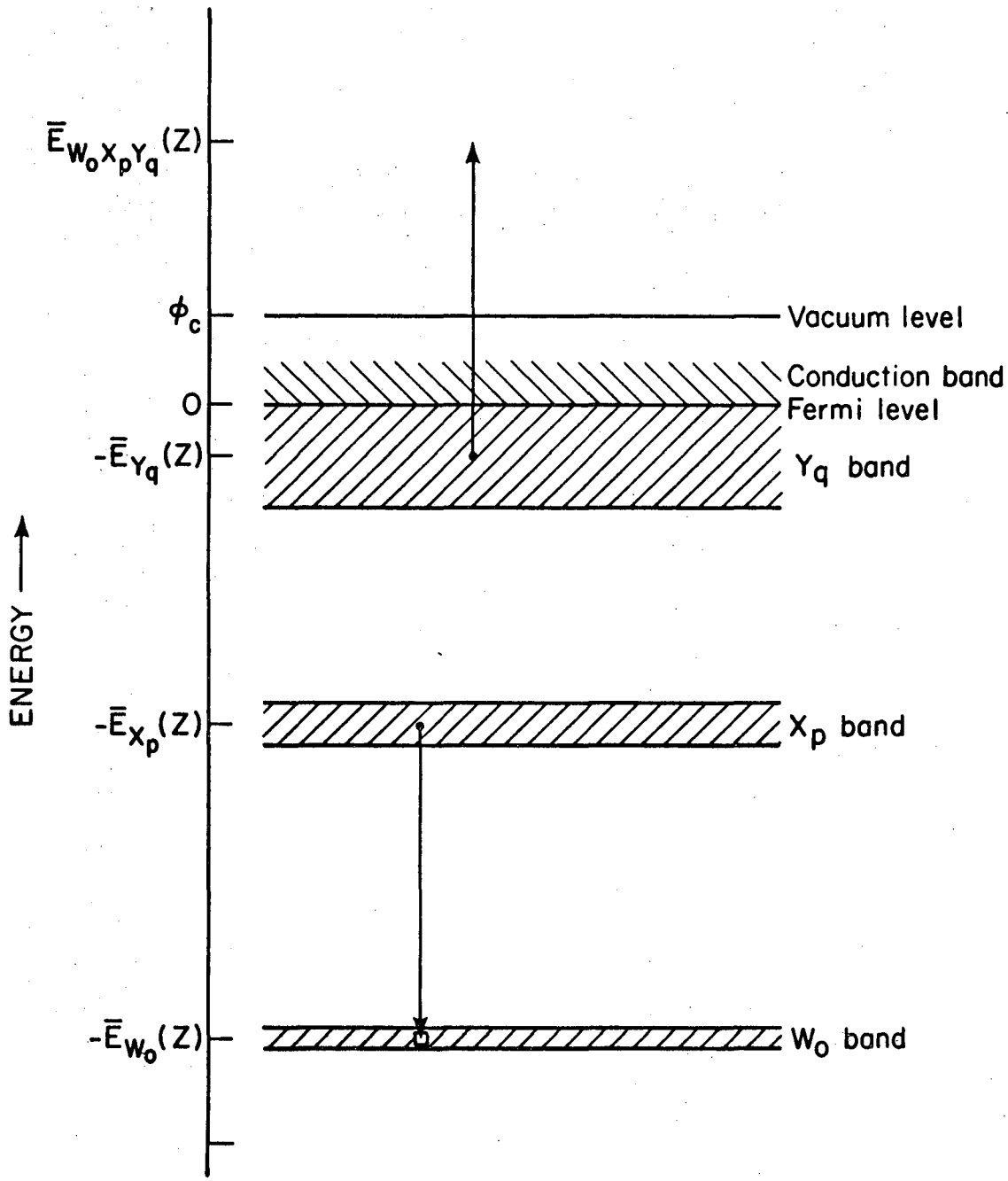

XBL 7012-7160

Fig. 1.

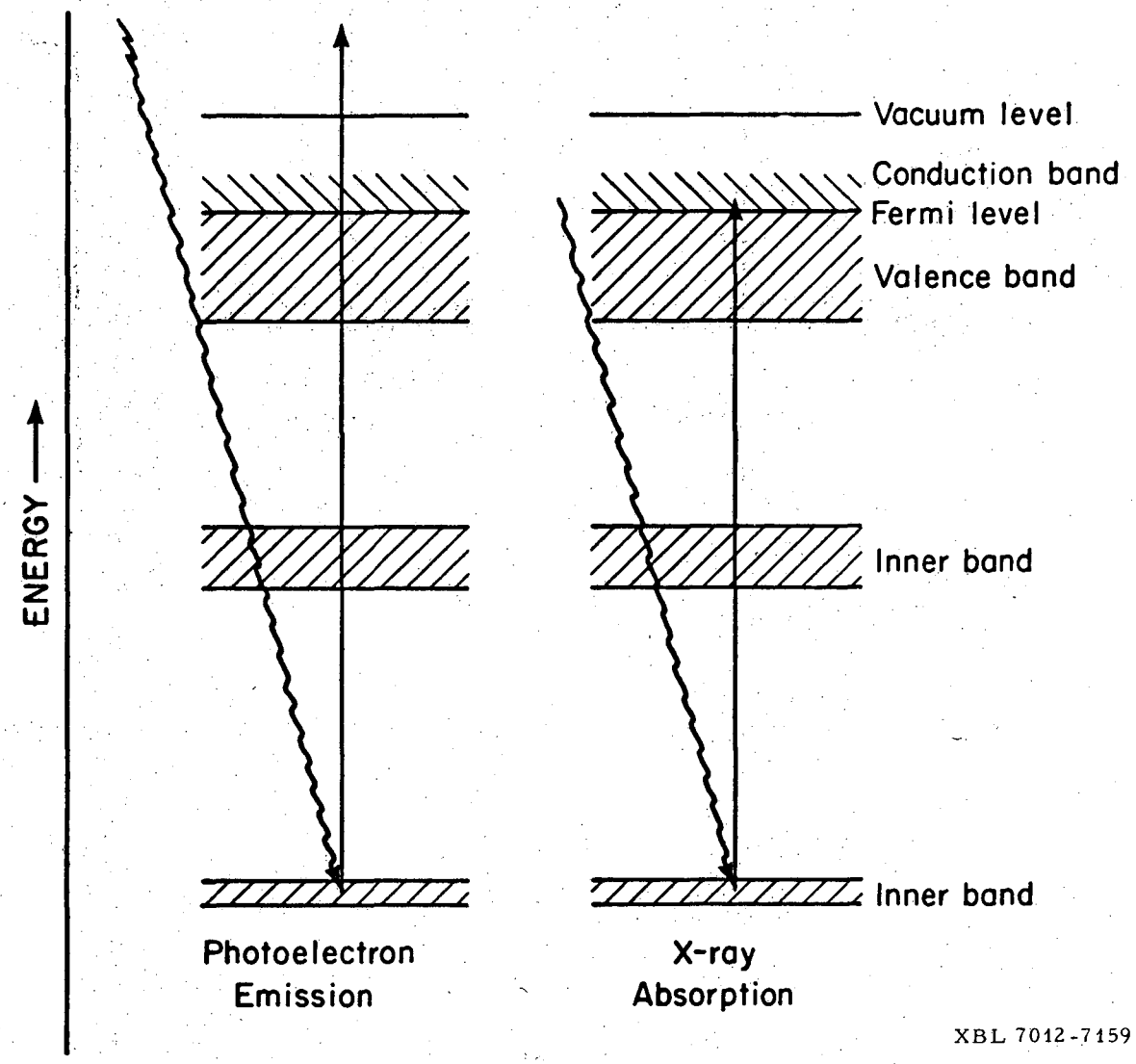
Vacuum level
Conduction band
Fermi level
Valence band
ENERGY
Inner band
Inner band
Photoelectron Emission
X-ray Absorption
XBL 7012-7159

Fig. 2.

Schematic Diagram of Auger Spectroscopy Apparatus.

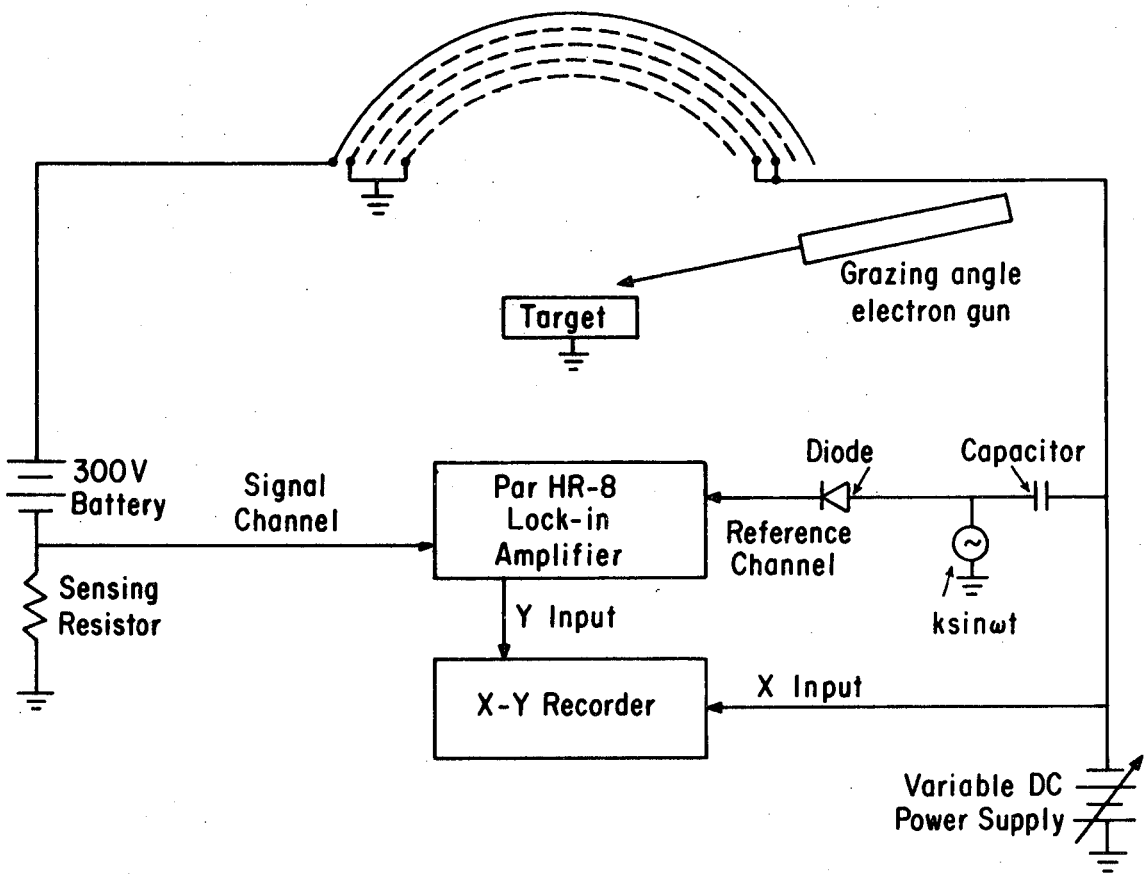

XBL 708-1722

Fig. 3.

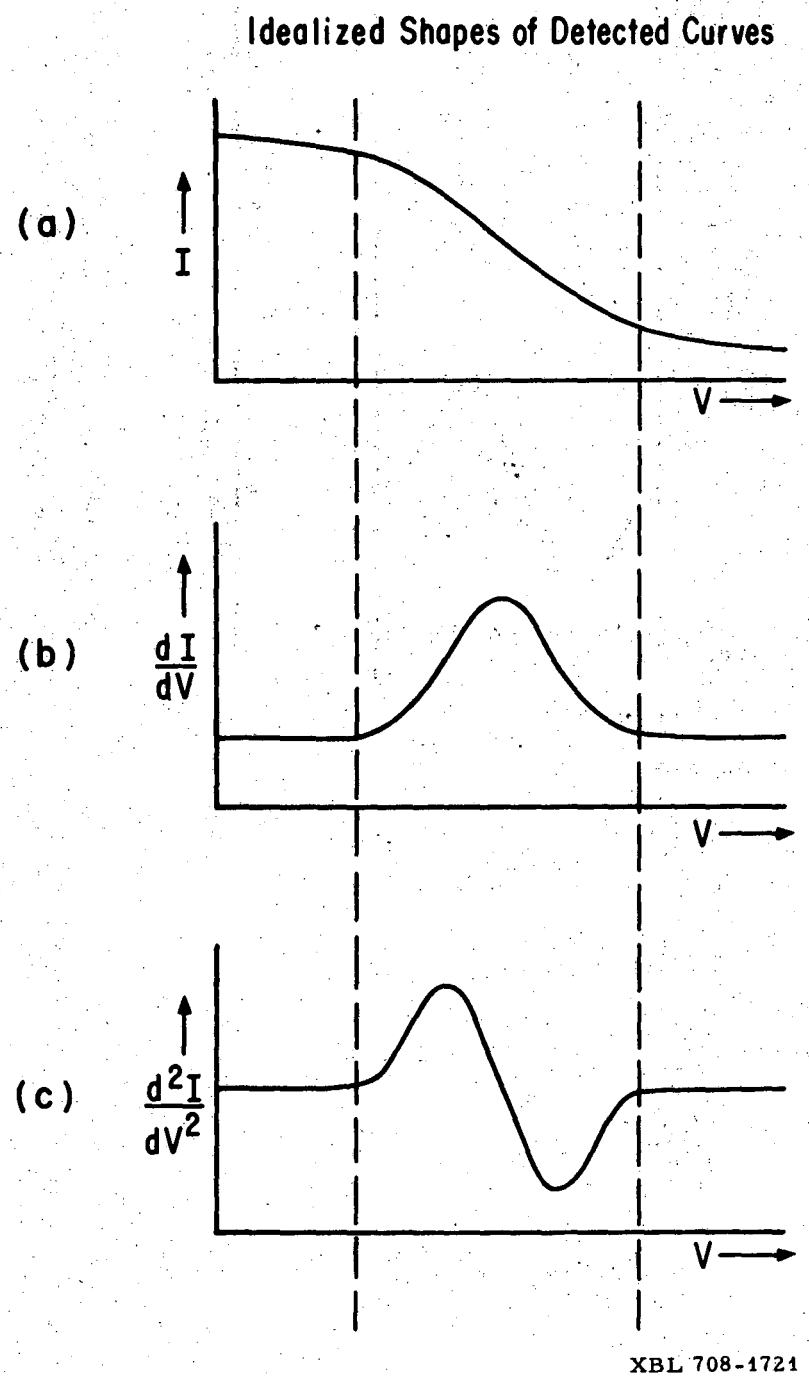
Idealized Shapes of Detected Curves
(a)
I
V
(b)
dI/dV
V
(c)
d²I/dV²
V
XBL 708-1721

Fig. 4.

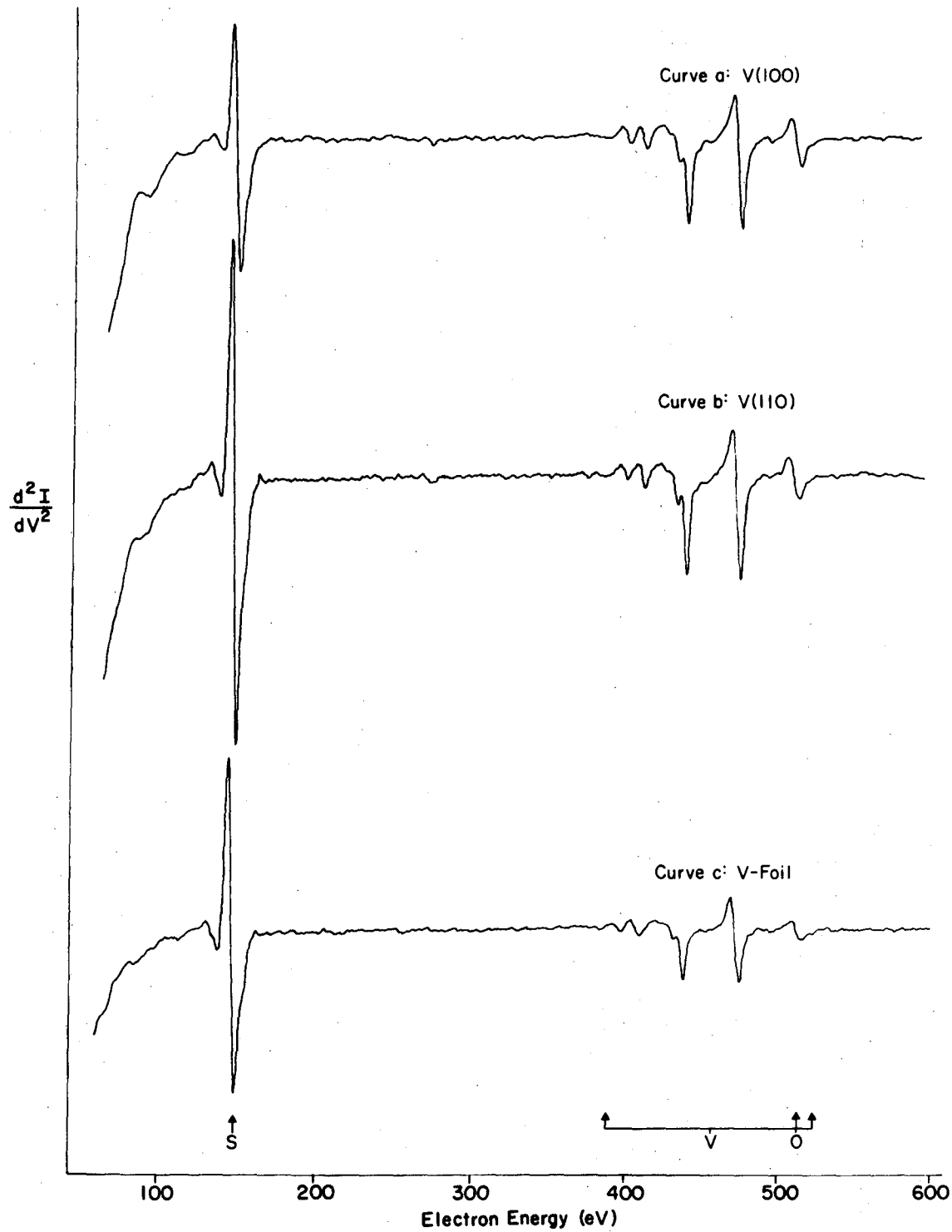

XBL 7012-7402

Fig. 5.

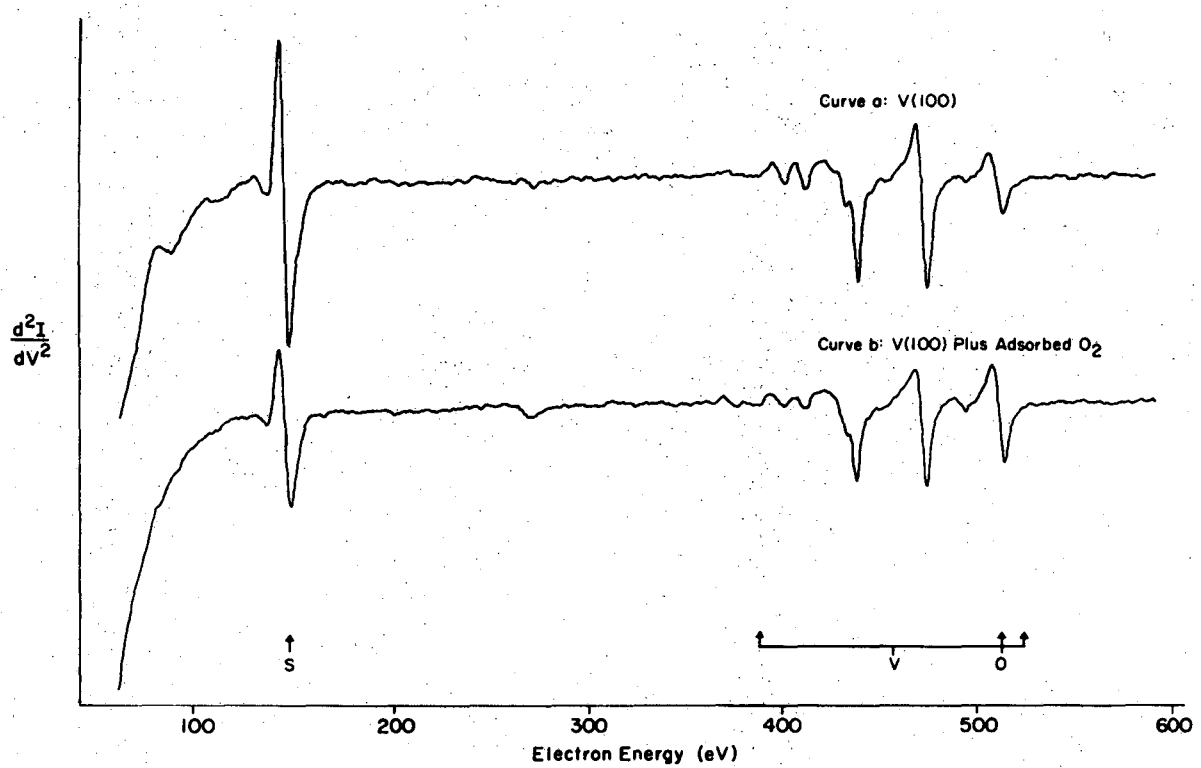

XBL 7012-7401

Fig. 6.

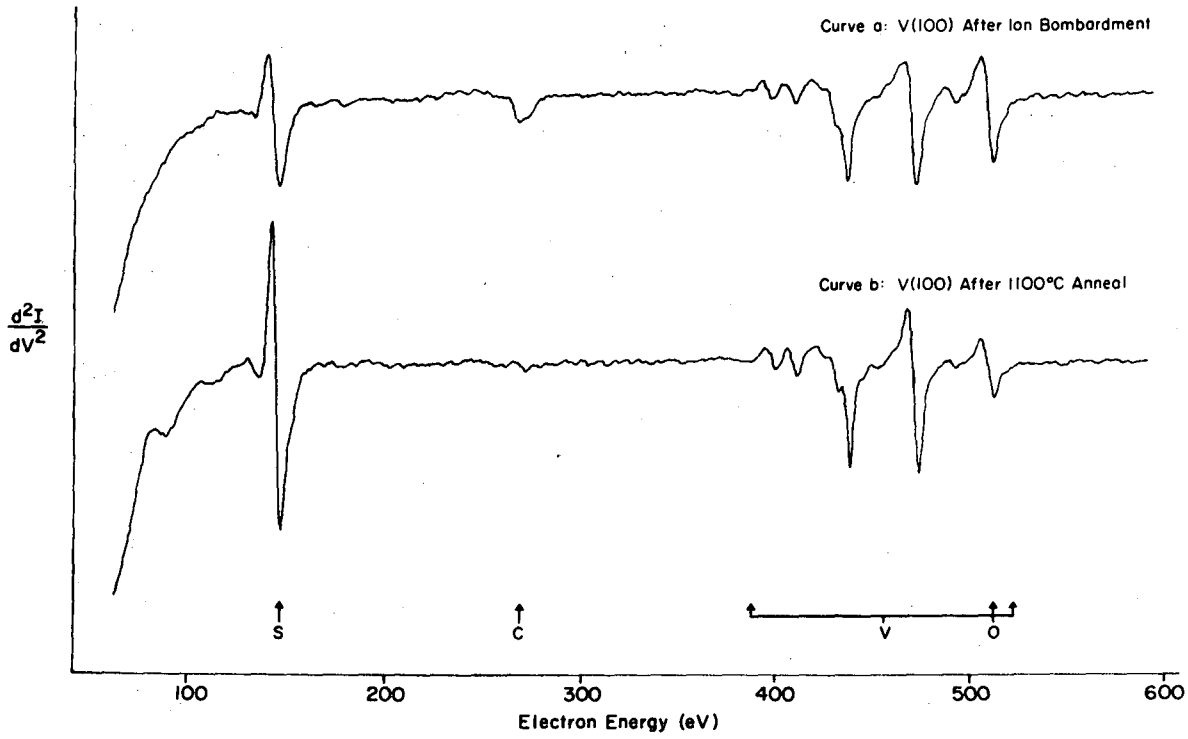

XBL 7012-7400

Fig. 7.

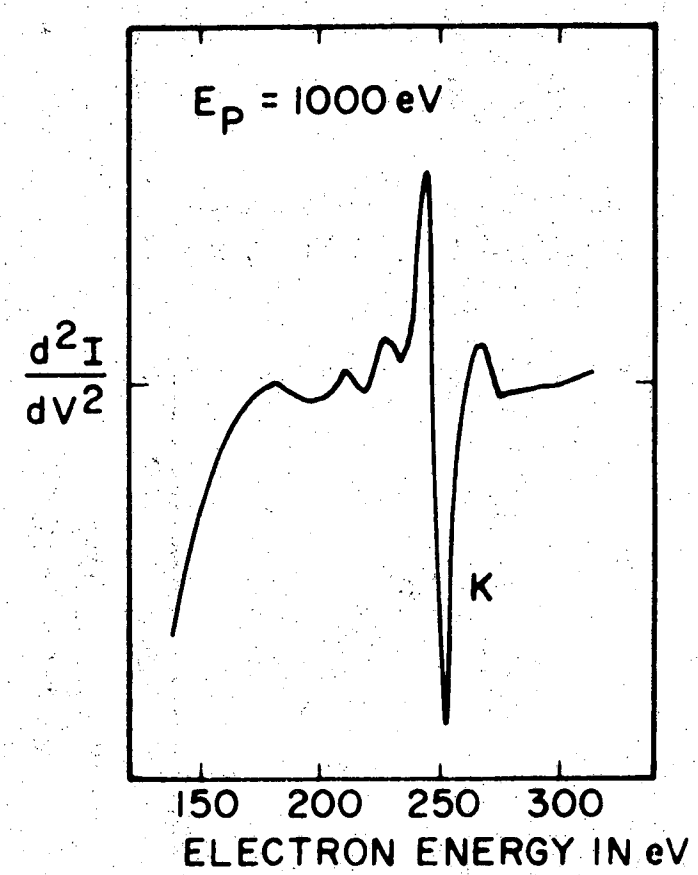

Fig. 8a.

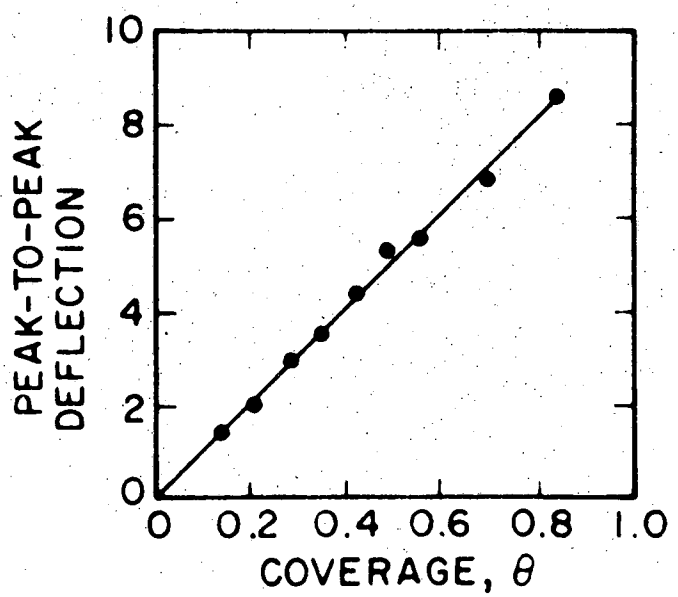

XBL 7012-7399

Fig. 8b.

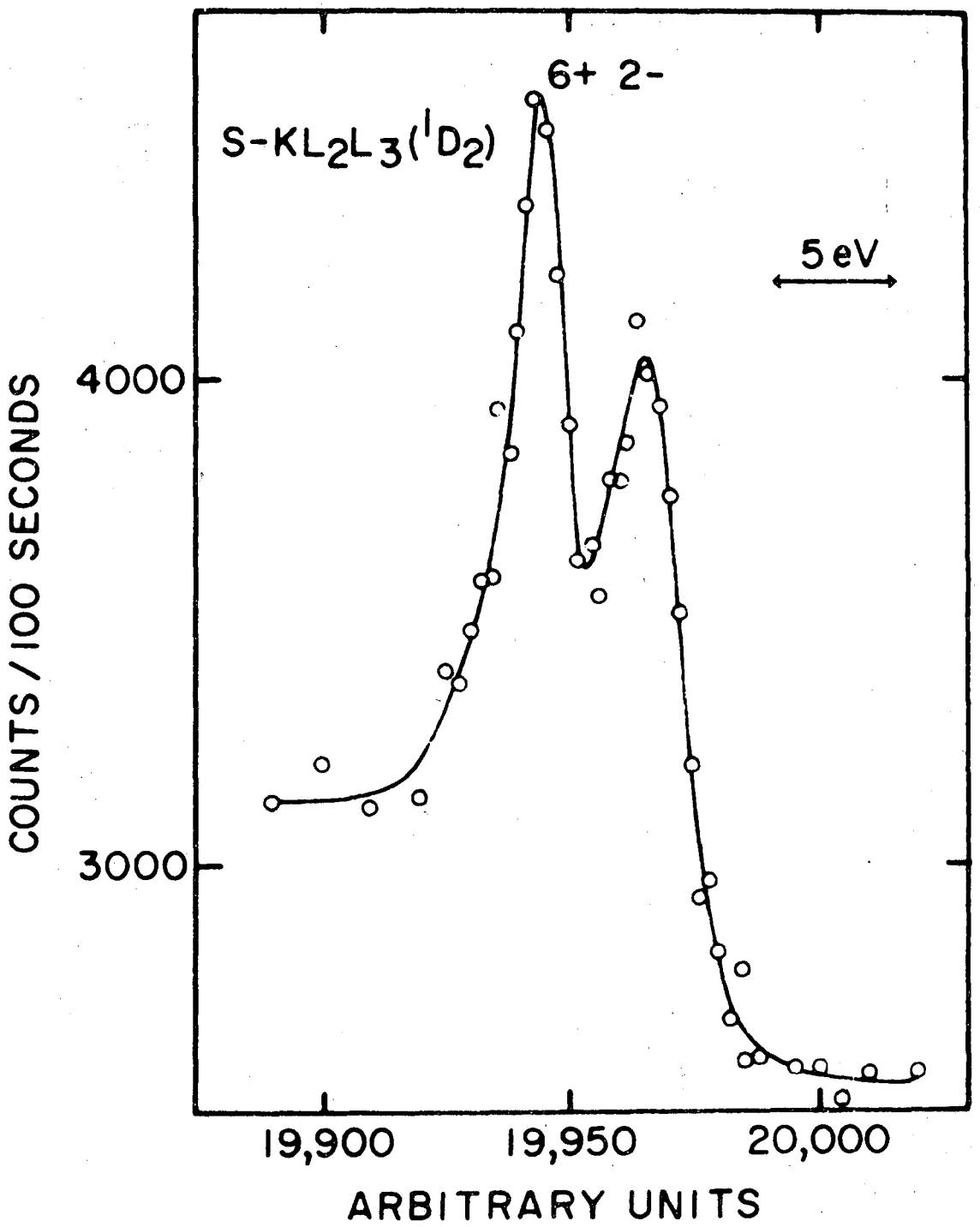

XBL 7012-7398

Fig. 9.

LEGAL NOTICE

This report was prepared as an account of Government sponsored work. Neither the United States, nor the Commission, nor any person acting on behalf of the Commission:

A. Makes any warranty or representation, expressed or implied, with respect to the accuracy, completeness, or usefulness of the information contained in this report, or that the use of any information, apparatus, method, or process disclosed in this report may not infringe privately owned rights; or

B. Assumes any liabilities with respect to the use of, or for damages resulting from the use of any information, apparatus, method, or process disclosed in this report.

As used in the above, "person acting on behalf of the Commission" includes any employee or contractor of the Commission, or employee of such contractor, to the extent that such employee or contractor of the Commission, or employee of such contractor prepares, disseminates, or provides access to, any information pursuant to his employment or contract with the Commission, or his employment with such contractor.

TECHNICAL INFORMATION DIVISION
LAWRENCE RADIATION LABORATORY
UNIVERSITY OF CALIFORNIA
BERKELEY, CALIFORNIA 94720